



# Data fusion of multi-sensor for IOT precise measurement based on improved PSO algorithms

Wen-Tsai Sung\*, Ming-Han Tsai

Department of Electrical Engineering, National Chin-Yi University of Technology, No. 57, Sec. 2, Zhongshan Rd., Taiping Dist., Taichung 41170, Taiwan

## ARTICLE INFO

### Keywords:

Internet of things  
Particle swarm optimization  
Data fusion  
RFID  
Wireless sensor network

## ABSTRACT

This work proposes an improved particle swarm optimization (PSO) method to increase the measurement precision of multi-sensors data fusion in the Internet of Things (IOT) system. Critical IOT technologies consist of a wireless sensor network, RFID, various sensors and an embedded system. For multi-sensor data fusion computing systems, data aggregation is a main concern and can be formulated as a multiple dimensional based on particle swarm optimization approaches. The proposed improved PSO method can locate the minimizing solution to the objective cost function in multiple dimensional assignment themes, which are considered in particle swarm initiation, cross rules and mutation rules. The optimum seclusion can be searched for efficiently with respect to reducing the search range through validated candidate measures. Experimental results demonstrate that the proposed improved PSO method for multi-sensor data fusion is highly feasible for IOT system applications.

© 2012 Elsevier Ltd. All rights reserved.

## 1. Introduction

Internet of Things (IOT) installs various sensors in each physical device in a network system. These elements include radio frequency identification (RFID), global positioning system (GPS), and wireless sensors network (WSN) technology [1]. The sensors are linked via the Internet or are wireless. Using remote control allows the sensors elements to communicate with individuals. IOT generally uses a wireless sensor network that features a comprehensive perception, with a reliable delivery up to the handle. IOT can easily monitor the location of supplies and equipment to achieve identification and transparent management of items, with positive control and anti-theft features. IOT applications can be found in medical, transportation, services, home, factories, and cities, reflecting the broad commercial applications for this technology [2].

In an IOT system, multi-sensor data fusion issues such as node signal processing, WSN localization, anti-collision and information-aggregation are often formulated as optimization subjects. Based on improved particle swarm optimization (PSO), this work attempts to comply with the moderate memory and computational resources requirements, while producing acceptable results for implementation on an individual sensor node. As a swarm based intelligence optimization approach, PSO addresses optimization topics by simulating the social behavior of bird flocks. PSO is a conventionally adopted multi-dimensional optimization procedure. Ease of implementation, high solution quality, computational efficiency and speed of convergence are the strengths of PSO [3]. PSO applications in multi-sensor data fusion are abundant in the literature. Based on improved PSO, this work increases the measurement radio effect precision for data fusion in IOT system computing.

Extensively adopted in the optimization field, PSO is a mathematical basis for solving a variety of multi-sensor data fusion problems to optimize the solution approach. Inspired by the foraging behavior of birds, Kennedy and Eberhar created the PSO algorithm in 1995. Following several experimental studies, Angeline found that the PSO algorithm can solve typical function

\* Corresponding author. Tel.: +886 932926974; fax: +886 4 23924419.

E-mail addresses: [songchen@ms10.hinet.net](mailto:songchen@ms10.hinet.net), [songchen@nctu.edu.tw](mailto:songchen@nctu.edu.tw) (W.-T. Sung).

optimization problems. A promising area includes multi-objective optimization problems, system design, classification, pattern recognition, biological systems planning modeling, signal processing, decision-making and simulation. Successful applications include fuzzy controller design, shop scheduling, real-time robot path planning, image segmentation, EEG signal simulation, speech recognition, diagnosis and detection of moving target's burns [4].

Based on ZigBee technology, the IOT system establishes a measurement environment among various sensor nodes. ZigBee is an inexpensive, low power consuming, low transmission rate, short-range wireless transmission system. Generally defined in the IEEE 802.15.4 protocol standard, which also belongs to the IEEE 802.15.4 standard, this system separately defines the medium access control layer (MAC) and physical layer (PHY) as the underlying system [5]. The IOT system based on a ZigBee sensor network is widely anticipated to be extensively used in smart homes, medical care, factory monitoring, and environmental control. A promising solution to this challenge is to employ the IPSO on the multi-sensors data fusion for IOT precise measurement. Through the improved PSO method, the measurement sensor results confirm the multi-objective expression data association problem for a class of combinatorial optimization problems to solve constraints. This approach is quite reasonable in some sensor elements in which the sensor's measurement result is derived from the applied data fusion and control theory. In the IOT system experimental analysis that we proposed, an improved PSO algorithm allows for more accurate measurement results in the number of multiple wireless sensors.

## 2. Literature survey

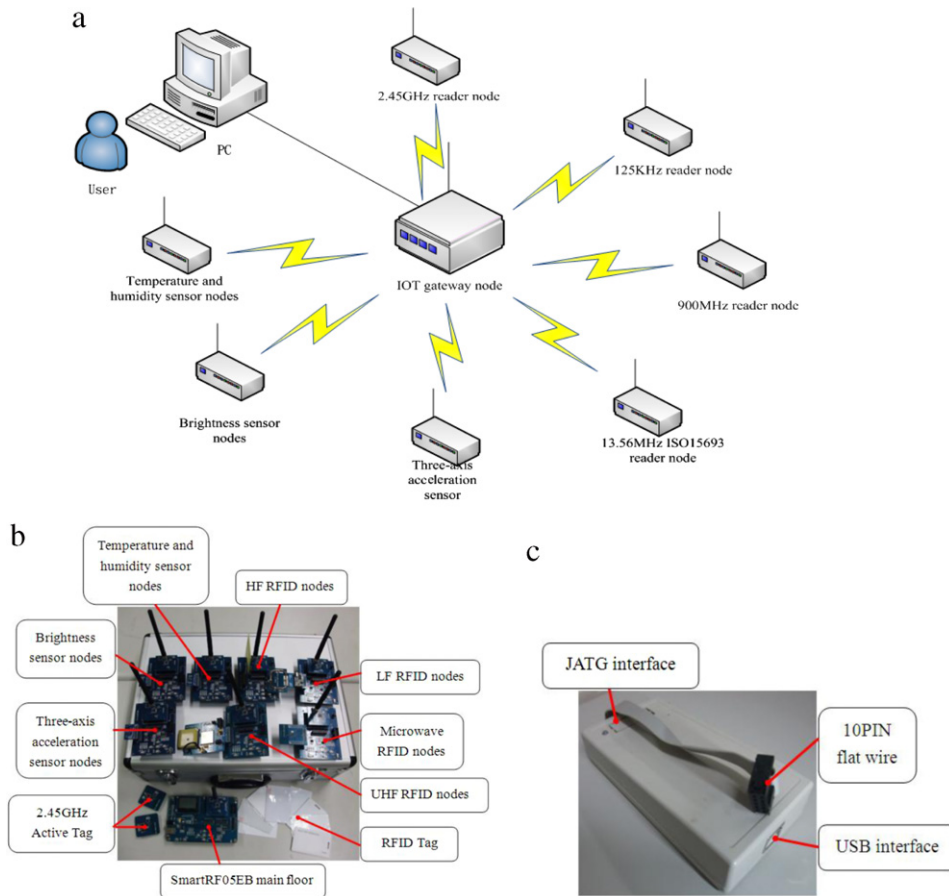
Owing to faster convergence rates, the particle swarm optimization-based genetic algorithm is simple, easy to understand, easy to implement, and often easier than the genetic algorithm (GA). Although more efficient, this algorithm fails to deal effectively with high dimensional problems [6]. The PSO algorithm is likely to degrade in several local minimum points. Many attempts have been made to enhance PSO algorithm performance, (further details can be found in [7–9]). Shi (1998) developed an adaptive inertia factor for the particle swarm optimization algorithm. Shi (2001) further proposed using the fuzzy rules algorithm to dynamically modify the inertia factor. While drawing on the concept of genetic algorithms, Angeline (1998) proposed a particle swarm optimization algorithm hybrid. Lovbjerg (2001) further proposed particle swarm optimization breeding [10]. Vanden Bergh (2001) proposed particle swarm optimization algorithm collaboration with the notion of using particles of  $K$  independent groups in the  $D$ -dimensional target-space dimension in different directions to search global optimization. Kennedy (1997) designed a discrete binary version of the particle swarm optimization algorithm. Clerc (2000) applied a PSO algorithm to the traveling salesman problem (TSP) and achieved satisfactory results [11]. Vanden Bergh (2002) developed an effective approach to ensure fast PSO algorithm convergence. This strategy incorporates a new global best particle update equation. The position equation of a particle is set to the global extreme point, making it near the global best position to generate a random search, while other particles remain updated with the original equation. Based on a Gaussian variation, Natsuki (2003) improved the ability of the proposed particle swarm optimization algorithm to jump out of local convergence.

Many works have attempted to improve the PSO algorithm since 2000. Notable examples can be found in [12,13]. Xu (2000) attempted to improve upon the fuzzy logic system particle swarm optimization self-learning algorithm. Wang (2003) adopted the standard PSO algorithm to increase the particle location update equation using the integral control idea. Integral control of each particle's fitness value determines the particle position changes, which can improve the ability to avoid local minima. Gao (2004) examined the organism immune system. The immune system incorporates an immune information processing mechanism into the PSO algorithm. The Harbin Institute of Technology developed a PSO algorithm based on chaotic thinking in 2005, which used a fast convergence PSO algorithm and factors such as chaotic transport ergodicity and randomness, to improve the standard PSO algorithm. Wu (2005) proposed a multi-objective optimization scheme to derive the improved PSO algorithm by using information transmission of the PSO algorithm. A multi-objective evolutionary algorithm, commonly used in archiving technology is introduced using environmental selection of the SPEA2 algorithm and matching options strategies, subsequently allowing the entire group to maintain an appropriate selection pressure in the Pareto optimal solution set convergence [14,15].

## 3. IOT system architecture and development platform

Fig. 1 illustrates the experimental development of the IOT system architecture. This study proposed a system using ZigBee CC2530 and RFID to constitute the Internet of Things. The IOT system hardware consists of a main board and seven cell base boards, as well as various sensors and RFID modules. The hardware components communicate with each other through wireless transmission. Each node in the data collection is sent messages to the key points of things and, finally, by computer display data and information processing. The battery plate can be viewed as a condensed version of the main board, by using two 1.5 V batteries for the power supply. Consequently, the mobility is significantly enhanced. Moreover, the IOT system can be used as a router or end device.

Fig. 1 shows the system architecture diagram of the key points of things, which is placed in the main board. The main board interface has a  $128 \times 64$  dot matrix font files LCD, UART to USB interface, LED indicator, user buttons, and user I/O area. In Fig. 1(b), the IOT experimental development platform uses three sensors: light, temperature and humidity, and a three-axis sensor. The sensor is installed in the battery plate as sensor nodes. IOT experimental simulation includes sensor module



**Fig. 1.** (a) IOT system architecture. (b) Experimental simulation platform of IOT. (c) Debugger multi emulator.

and RFID for integration. RFID tags have four frequency bands: 125 kHz LF RFID modules, 13.56 MHz HF RFID Module, 900 MHz UHF RFID Module, and 2.4 GHz RFID module [16].

Fig. 1(c) shows the development platform debugger multi-emulator device, SmartRF05EB the main floor and the floor and the computer link SmartRF05BB battery. The device uses JATG Interface 10PIN flat wire transfer through the debugger multi emulator after the USB interface. The computer is then connected to burn the compiled code and the node to the main floor panels in order to complete the burn after the experiment can be simulated.

Fig. 2(a) shows the SmartRF05EB development platforms in the main board; the device belongs to the IOT things in the ZigBee network coordinator. Interface with a  $128 \times 64$  dot matrix font files LCD, UART to USB interface, LED indicator, user buttons, user I/O area and other rich features. The SmartRF05EB main floor houses three power supplies: the DC interface power supply, USB interface power supply and battery-powered. A debugger multi emulator uses a USB interface connected to a computer. The code is developed after burning to the main backplane. The star network, tree network, and mesh networking are supported by ZigBee protocol. The main floor can also be connected to a sensor module and the RFID module, in which the user can be based on different needs, which is an additional expansion.

Fig. 2(b) shows the Development Platform SmartRF05BB battery plate. SmartRF05EB on the main floor with functions in SmartRF05BB battery also has a main floor in the bottom part of the function. The battery plate can be regarded as a condensed version of the main floor. The main floor of the LCD and USB serial interface switch simplification enhances mobile battery-powered performance. Following the installation of the CC2530EM battery plate, all ZigBee networks can be used as a router or end device. CC2530EM has a CC2530 chip and a 32 MHz oscillator, capable of receiving various sensor data types and RFID modules, transmitted by the antenna back to the computer through the main floor display processing. Fig. 3 shows various sensor types and RFID modules [17].

#### 4. Improved PSO algorithm

In the multi-sensor data fusion system, data aggregation is based on a common source of a similar nature. Certain allocation strategies are grouped into multi-sensor observations. The correlation is even more complex owing to false alarms and missed uncertainty processes such as an observation. Solutions for these complex issues are the nearest neighbor

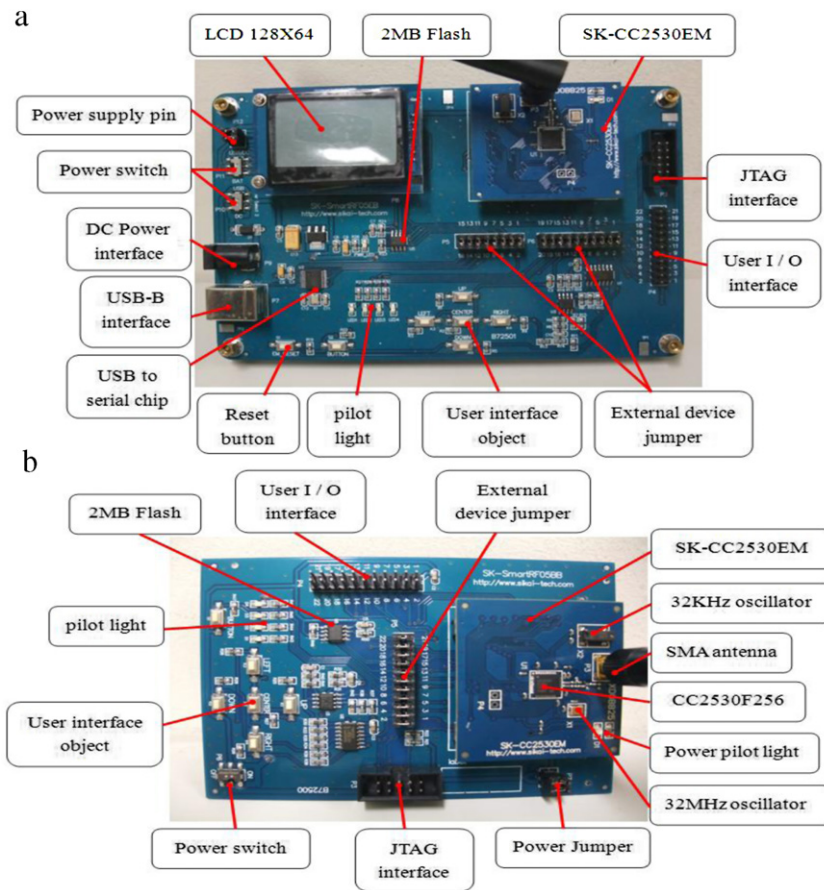


Fig. 2. (a) SmartRF05EB main board. (b) SmartRF05BB battery plate.




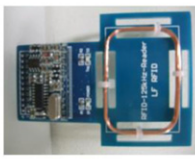
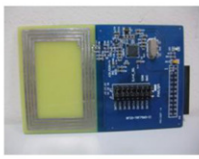
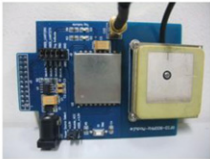

sensor module			
	Brightness	Temperature and humidity	Three-axis acceleration
RFID module			
	125KHz LF	13.56MHz HF	900MHz UHF
			
			2.4GHz microwave

Fig. 3. Various sensor types and RFID modules.

method and probabilistic data association algorithm, which many works assume are algorithm and multi-dimensional assignment algorithm. This work presents a novel PSO algorithm to solve a multi-dimensional distribution problem. Measurement sensor results confirm the multi-objective expression data association problem for a class of combinatorial optimization problems to solve constraints. Its particle encoding, initialization, crossover and mutation development strategies achieve a more intensive environment of clutter and dense multi-target data association, after the last associated

fusion measurement with satisfactory results. Simulation results demonstrate the superiority of this algorithm in optimum fitness and data fusion error probability [18].

Assume that there are  $N_s$  sensors from the surveillance area scan measurements of  $S$ , in which each sensor has a certain number of measurements, but not necessarily equal to the actual number of targets. In the current problems  $S = N_s$ , in which each sensor has a scan, a scan assumes that all sensors are functioning simultaneously. The purpose of the data is associated with a measurement of  $S$  estimated target states.

By assuming a multi-sensor data fusion environment, the target state equation and measurement equation are as follows:

$$X_i^{(k+1)} = \Phi(k + 1|k)X_i(k) + G(k)W(k) \tag{1}$$

$$Z_{s_i_s}(k) \begin{cases} H(k)X_i(k) + V(k) \\ Y(k). \end{cases} \tag{2}$$

In Eq. (2),  $Z_{s_i_s}(k)$  measurements from the target  $i$  and clutter, where  $X_i(k)$  represents a target state vector  $i$ ,  $Z_{s_i_s}(k)$  denotes a sensor  $S$  measurements vector,  $W(k)$  and  $V(k)$  for the state noise and measurement noise respectively, are uncorrelated Gaussian white noise sequences, the  $\Phi(k + 1|k)$ ,  $G(k)$ , and  $H(k)$  are state transition matrix, input matrix and observation matrix, and  $Y(k)$  represents the observation area of a clutter. For each  $S$ -dimensional distribution associated with the  $S$  at time  $k$  from the sequence of  $n_s$  measurements,  $s = 1, 2, \dots, S$ . Assume that time  $k$  target  $i$  at real position is  $X_i(k)$ , Sensor  $s$  position is  $y_s(k)$ ,  $i$  measurement of the target  $Z_{s_i_s}(k)$ ,  $i_s = 1, 2, \dots, n$ . The above measurements may be due to either a real goal or a false target. The sensor provides the target at time  $k$  of the  $s$ -group to assign weights measured with the  $s$ -dimensional assignment algorithm in order to minimize the overall power. To simplify the missed computing due to incomplete measurements and interconnected goals,  $Z_{s_0}$  virtual measurement is added to each sequence. Also,  $s$  in the sequence is assigned to the target virtual measurement  $i$ ; this goal has not been detected by sensor  $s$ . From the target for  $i$ ,  $k$  moment time when the actual state  $x_i(k)$ ,  $S$ -set of measurements  $Z_{i_1 i_2 \dots i_s}$  (the measure that  $Z_{i_1} Z_{i_2} \dots Z_{i_s}$ ) of the likelihood probability (time omitted):

$$\wedge(Z_{i_1 i_2 \dots i_s} | i) = \prod_{s=1}^S \{ [1 - P_{D_d}]^{1-u(i_s)} [P_{D_s} p_{(Z_{s_i_s} | x_i)}]^{u(i_s)} \} \tag{3}$$

where:  $u(i_s)$  refers to the indicator function, i.e.

$$u(i_s) \begin{cases} 0 & i_s = 0 \\ 1 & \text{other.} \end{cases} \tag{4}$$

Measurements are either false alarms or irrelevant to this target. The probability that the likelihood

$$\wedge(Z_{i_1 i_2 \dots i_s} | i = \Phi) = \prod_{s=1}^S \left[ \frac{1}{\Psi_s} \right]^{u(i_s)} \tag{5}$$

where:  $\Psi_s$  represents the size of the sensor probe field (the area of two-dimensional, three-dimensional as the volume),  $i$  is associated with the target  $S$  – the right group of log likelihood probability:

$$c_{i_1 i_2 \dots i_s} = - \ln \frac{\wedge(Z_{i_1 i_2 \dots i_s} | i)}{\wedge(Z_{i_1 i_2 \dots i_s} | i = \Phi)}. \tag{6}$$

However, if Eq. (1) of  $X_i(k)$  is unknown, then by its maximum likelihood estimation rather than that:

$$\hat{x}_i = \arg \max_{x_i} \wedge(Z_{i_1 i_2 \dots i_s} | i). \tag{7}$$

This allows Eq. (6) into the normalized likelihood ratio. Take the (3) and (7) into (6),  $S$ -group  $i_1, i_2, \dots, i_s$  and the target measurement rights related to alternative,

$$c_{i_1 i_2 \dots i_s} = \sum_{s=1}^S \left\{ [u(i_s) - 1] \ln(1 - P_{D_s}) - u(i_s) \ln \left( \frac{P_{D_s} \Psi_s}{|2\pi R_s|^{1/2}} \right) + u(i_s) \frac{1}{2} [Z_{s_i_s} - H(x_i, y_{x_i_s})]^T R_s^{-1} [Z_{s_i_s} - H(x_i, y_{x_i_s})] \right\}. \tag{8}$$

The above equation attempts to identify the  $S$ -group maximum likelihood set. Therefore, each measurement is assigned to a goal and only one target, or judged as a false target and up to obtain each target in each sequence of a measurement. This distribution of the  $S$ -dimensional is re-grouped into,

$$J^* = \min_{\rho_{i_1 i_2 \dots i_s}} \sum_{i_1=0}^{n_1} \sum_{i_2=0}^{n_2} \dots \sum_{i_s=0}^{n_s} c_{i_1 i_2 \dots i_s} \rho_{i_1 i_2 \dots i_s}. \tag{9}$$

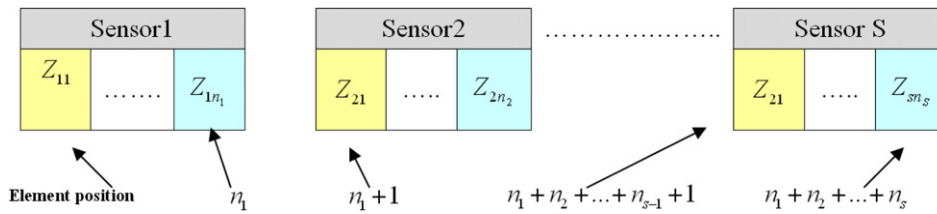


Fig. 4. Schematic diagram of particle code for link list of multi-sensors data fusion.

Meet:

$$\begin{aligned}
 &\sum_{i_2=0}^{n_2} \cdots \sum_{i_s=0}^{n_s} \rho_{i_1 i_2 \cdots i_s} = 1, \quad i_1 = 1, 2, \dots, n_1 \\
 &\sum_{i_1=0}^{n_1} \sum_{i_3=0}^{n_3} \cdots \sum_{i_s=0}^{n_s} \rho_{i_1 i_2 \cdots i_s} = 1, \quad i_2 = 1, 2, \dots, n_2 \\
 &\sum_{i_1=0}^{n_1} \cdots \sum_{i_{s-1}=0}^{n_{s-1}} \rho_{i_1 i_2 \cdots i_s} = 1, \quad i_s = 1, 2, \dots, n_s
 \end{aligned} \tag{10}$$

where:  $\{\rho_{i_1 i_2 \cdots i_s}\}$  denotes a binary dependent variable, making the  $S$ -group if  $Z_{i_1 i_2 \cdots i_s}$  is associated with an alternative target which is  $\rho_{i_1 i_2 \cdots i_s} = 1$ , and 0 otherwise. Notably, the measurement does not only belong to the virtual target or clutter a constraint; it can also be repeated [19,20].

The improved PSO algorithm simulates birds of prey behavior to solve the optimization problem. First, the solution space is a random initialization of birds; birds of every known kind are used as the “particles”. The “particles” are mobile in the solution space. Following several iterations, the optimal solution is obtained. The particles perform data fusion computing by using the two “extremes” to renew itself during the each iteration. The first one is the optimal solution of the particle itself,  $p$ , the first two are present throughout the particle swarm to derive the optimal solution,  $g$ . While attempting to locate these two extremes, each particle is based according to their flight speed, to determine their own direction and distance.

The speed of the improved PSO formula is derived as follows:

$$v_{t+1} = w_0 v_0 + \eta_1 \text{rand}() (p_t - x_t) + \eta_2 \text{rand}() (g_t - x_t) \tag{11}$$

$$x_{t+1} = x_t + v_{t+1} \tag{12}$$

where  $v_t$  represents the first step of the particle velocity vector  $t$ ;  $x_t$  refers to the  $t$ -th step of the position of the particle;  $p_t$  denotes the  $t$ -th step to find the particle location of the optimum solution itself;  $g_t$  is the  $t$ -th steps population in which the best solution is located;  $w_0$  refers to inertia weight,  $\eta_1, \eta_2$  for  $p_t$  and  $g_t$  in order to adjust the relative importance of the parameters for the normal number, called the acceleration factor;  $\text{rand}()$  is  $[0, 1]$  random number. Generally the  $w_0$  takes  $(0, 1)$  random number; the  $\eta_1$  and  $\eta_2$  takes  $(0, 2)$  random number. If the IOT has  $S$  sensors, sensor  $s$  measurement of the particles encoded is shown in Fig. 4:

The total length of particle  $n_1 + n_2 + \cdots + n_{s-1} + 1$ , at  $k$  times the number of individual sensors and measurement, where  $Z_{1i}, Z_{2i}, \dots, Z_{Si}$ , which is assumed to be the same goal from the  $i$ -th sensor target to actual situation, is often missed and false measurements exist. Therefore, sensor  $s$  misses the target with  $Z_{s0}$ . By setting in particle number  $n_p$ , i.e. number of iterations  $n_{\max}$ , the overall algorithm execution is as follows:

- (a) Initialize the particle swarm, with each particle assigned to a random initial solution and the exchange of random probability and mutation probability calculation based on the current position of the particle fitness value. Also, set the current value of the individual to adapt to extreme  $p$ , global extreme  $g$ , while the number of iterations  $t < n_{\max}$  provides the number of iterations, the (b)–(f), when the system locates the optimum solution and the step is completed.
- (b)  $q_0$  and  $p_0$  of the particle cross derive a new solution  $q'_1$ .
- (c) The new solution  $q'_1$  and  $g$  cross obtain a new solution  $q''_1$ .
- (d) Variation of  $q''_1$  is  $q_1$ .
- (e) The fitness function calculation is based on the current solution, two positions due to changes in the amount of  $\Delta E$  fitness function. If  $\Delta E < e$  ( $e$  is deteriorated by allowing the scope of the objective function),  $\Delta E \leq 0$ , accept the new value of  $q_0 \leftarrow q$ ; otherwise, reject the assumption that the particle is still  $q_0$ .
- (f) If the particle has less than the current optimal fitness function value, this particle is updated to the current best particle  $p$ . If the particle has less than the global optimum fitness value, this particle is updated to the current best particle  $g$ .

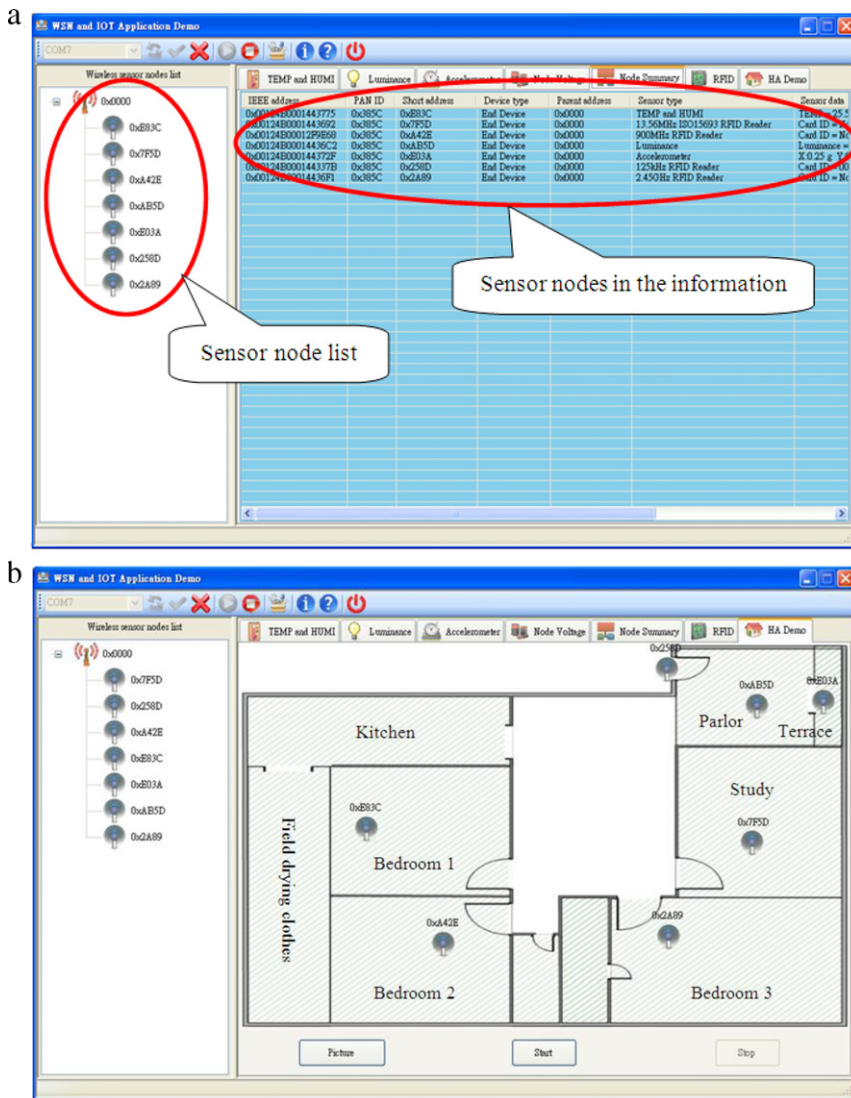


Fig. 5. (a) Communication interfaces. (b) Layout node.

### 5. Simulation and analysis results

The ZigBee CC2530 chip with RFID for IOT was used for the experimental simulation work. The program was compiled using IAR Embedded Workbench software and then coded. A development board through the JTAG Debugger multi emulator interface to the USB interface was connected to the computer. The code was then burned to the battery plate and sensing element of each sensor node according to the node type burned with the appropriate code. The experimental simulation environment is the general home environment. SmartRF05EB is the first development board via USB interface and the computer communication interface connection. The communication interface was chosen on ZigBee, the motherboard using a COM Port communication. The IOT system opens the sensor nodes and RFID module bottom of the battery power and emission signals back to the development board. The board receives the signal from each node displayed on the computer communication interface, as shown in Fig. 5(a).

The development board accumulates the sensor signals and RFID module. The communication interface displays the list of sensor nodes. Each node is set to the home environment in each region. Fig. 5(b) displays the living room, balcony, bedroom, study and door. The sensor node locations are determined using the free replacement demand. Sensor nodes can also be installed in the equipment and materials during application. Following completion of each node, the communication interface via the computer observes the status of the nodes.

During the simulation experiment, the sensor nodes in the living room set the brightness, sensing the living room illumination is abnormal. If the light intensity is below the set value, the system automatically records the time that the exception occurs. Fig. 6(a) shows the sensed data sent to the chart. The chart starts sensing changes in the light intensity

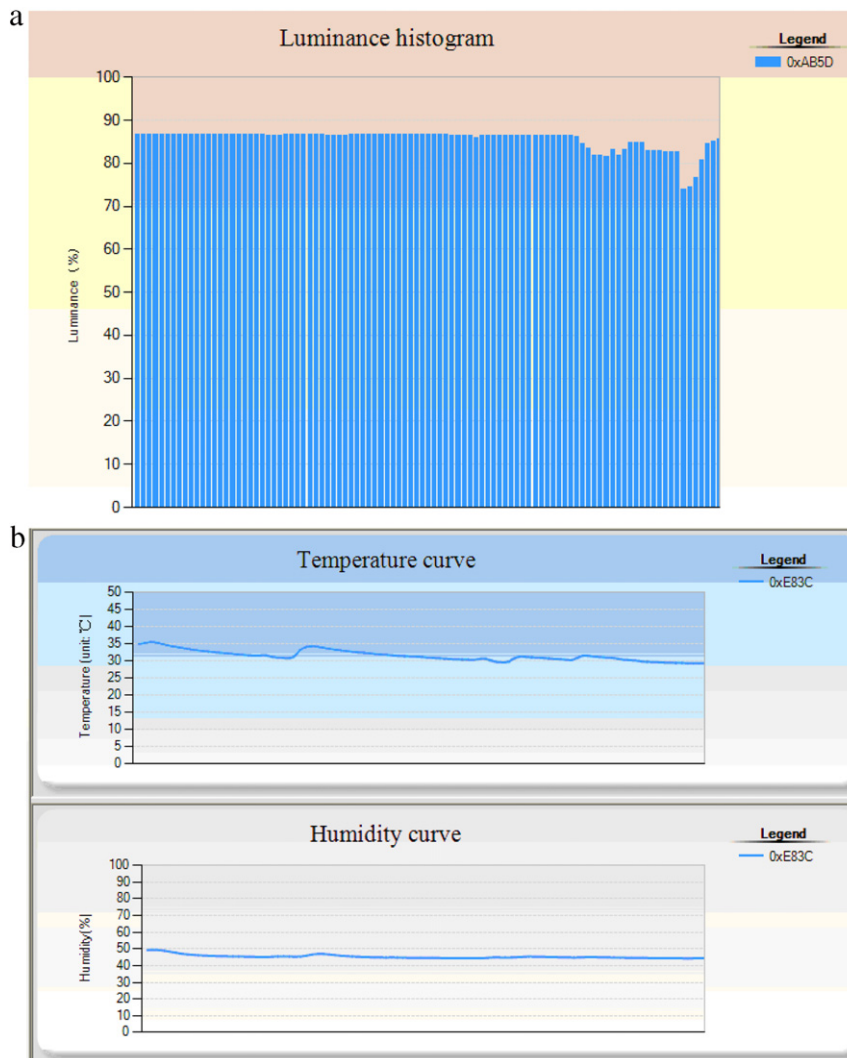


Fig. 6. (a) Optical sensor data. (b) Temperature and humidity curves.

at 87%. However, if a hand or items obscure the light sensor, the sensor immediately reduces the data percentage. Therefore, if the location of light sensors' installation is correct, selecting a shelter in the place of interference is unnecessary, therefore, the light sensor can sense ambient light.

Temperature and humidity sensor nodes are set in the master bedroom to sense the temperature and humidity. If the temperature and humidity are below the set value and the control device maintains a comfortable indoor environment, those values are corrected. Re-use development board temperature and humidity sensor nodes gather data to display the communication interface graphically. Fig. 6(a) shows the changes in temperature and humidity nodes. Fig. 6(b) illustrates changes in temperature and humidity data in a normal sense to maintain the initial temperature sensor at 26 °C and humidity sensor ratio at 45%. However, Fig. 6(b) shows a hair dryer or other items to maintain interference to make sense of data that produced significant changes in temperature sensing temperature gradually from 26 to 35 °C, along with changes in humidity from 45% to 50%. When human interference is stopped, the data is a period of time that quickly returns to a normal temperature and humidity condition, and does not interfere with and reduce the sensing accuracy.

Simulation experiments are performed using three-axis sensor nodes to sense the balcony; the nodes can pick up an empty balcony and these nodes are installed in the equipment and materials. X, Y, Z axis sensing equipment and materials stability. The sensor data are then sent back to the development board. These sensors receive X, Y, Z axis tilt on the development board. Fig. 7(a) shows the graph axis sensing in the communications interface. Our results clearly observe the tilt position, with adjustments finally made for improvement of efficiency. Based on the X-axis movements, tilting the sensor board to the right causes the X-axis values to rise, a tilt to the left decreases the X-axis value; the Y-axis values are the same and the Z-axis tilt value is also affected. Y-axis movements of the sensor board tilt down, causing a drop in the Y-axis values. Tilting up the Y-axis values causes a rise in weak sense environmental changes. The Z-axis value is also affected due



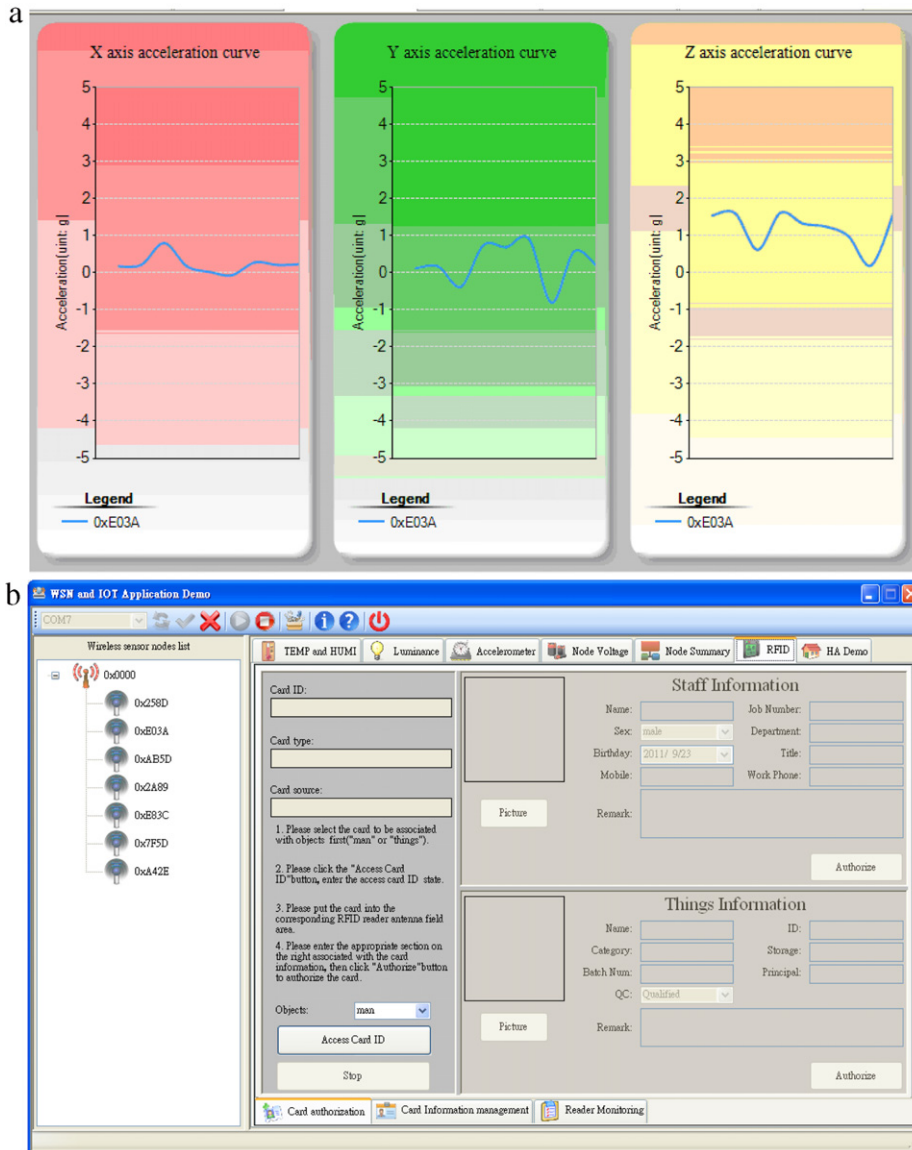


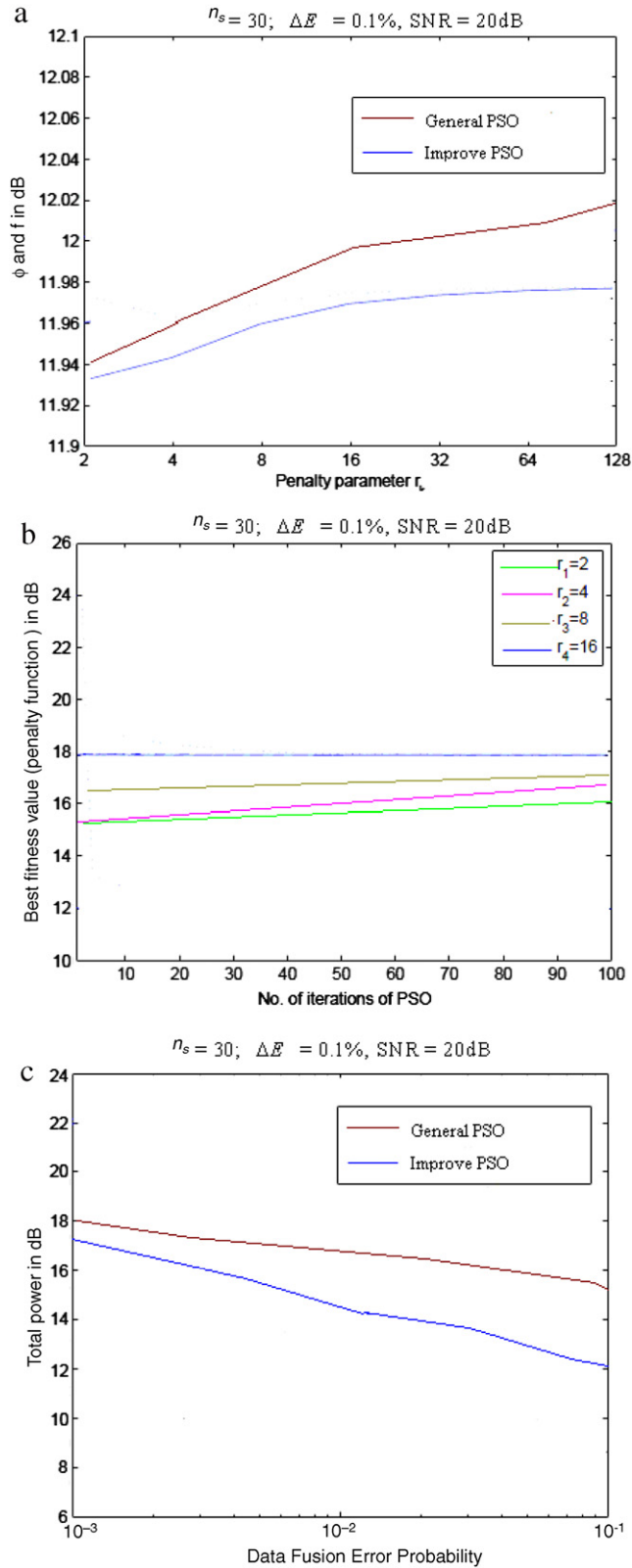
Fig. 7. (a) Three-axis sensing graph. (b) RFID configuration interface.

to tilting up and down. Z-axis movements and horizontal values are 1.5 g; when the Z-axis in the vertical is at 90° and -90°, the value is from the 1.5 g down to 0.5 g; when the Z-axis level of state is anti -180° and -180°, the value dropped by 1.5–0.5 g. Fig. 7(a) shows the tri-axis accelerometer with changes in the various environmental situations.

In addition to sensors, the experimental simulations involve four groups of RFID modules. Sensors on the IOT system are set at the door, study and second bedroom, in which RFID 125 kHz LF RFID module contains the module, 13.56 MHz HF RFID Module, 900 MHz UHF RFID Module, 2.4 GHz RFID. RFID cards, which are required to perform authorization via a communication interface set. Fig. 7(b) illustrates the authority to set the interface, login using the name, job number, title, and the data message as well. The user can then update the information and record the card reader to read the time, identity and type.

This study illustrates the possible performance gains with the derived optimal multi-sensor precise measurement for the data fusion allocation scheme. The fading coefficients  $Z_{s0}$  of the channel between the sensors and the fusion center are assumed to be the total length of the particle  $n_1 + n_2 + \dots + n_{s-1} + 1$  distributed with a unit mean (Fig. 8).

In the IOT system experimental analysis, this work assumes that  $n_s$  is equal to 30, 80, 160, and 250 as the number of multiple wireless sensors. According to Table 1, with a larger number of sensor signals, the proposed improved PSO algorithm allows for more accurate measurement results (compared with the normal mode and the conventional PSO), especially when the experimental results are more obvious after  $n_s > 160$  [21,22].



**Fig. 8.** Convergence of exterior penalty function based improved PSO: multi-sensor data fusion error probability is below 0.01%. (a) Optimum fitness returned for improved PSO iterations for a given penalty parameter. (b) Convergence of penalty function to the original optimization problem. (c) PSO data fusion error probability is improved when observations are correlated with each other ( $n_s = 30$ ;  $\Delta E = 0.1\%$ ; SNR = 20 dB).

**Table 1**

Comparative analysis of calculated various initial populations and iterations in IOT experimental ( $n_s = 30, 80, 120, 160, 250$ , improved PSO algorithm (IPSO)).

$n_s$	Approaches	Average error rate %	Convergence %	Iterations %	Success %
30	Non-PSO	<0.001	97.3	53.3	93.2
	PSO	<0.001	99.1	53.2	91.5
	<b>IPSO</b>	<b>&lt;0.001</b>	<b>99.0</b>	<b>54.1</b>	<b>91.5</b>
80	Non-PSO	<0.12	92.2	71.3	89.2
	PSO	<0.05	90.0	70.9	89.8
	<b>IPSO</b>	<b>&lt;0.01</b>	<b>96.2</b>	<b>62.4</b>	<b>90.1</b>
160	Non-PSO	<0.42	80.8	74.0	87.3
	PSO	<0.31	82.6	69.1	89.5
	<b>IPSO</b>	<b>&lt;0.20</b>	<b>94.2</b>	<b>68.6</b>	<b>94.5</b>
250	Non-PSO	<0.93	68.5	81.3	83.8
	PSO	<0.68	82.4	78.2	89.6
	<b>IPSO</b>	<b>&lt;0.32</b>	<b>86.5</b>	<b>73.2</b>	<b>93.1</b>

## 6. Conclusions and future work

The IOT system implements ZigBee wireless sensor network technology combined with RFID technology to monitor the status of a given region. This work proposes better IOT system improvement strategies than the traditional optimal solution does. The general PSO multi-sensor data fusion computing error probability is below 0.01%. The improved PSO IOT system is reliable owing to its simplicity, high solution quality, rapid convergence and insignificant computational burden, which is superior to existing PSO approaches. The iterative nature of the improved PSO algorithm is highly promising for use in high-speed real-time applications, especially if optimization must be carried out frequently.

This work develops a friendly interface that can be set to sensor node monitoring standards with other devices in order to enhance the control area status. RFID technology in the IOT system allows for controlled access in the movement of goods. Individuals are logged based on the RFID gag system. The RFID tag provides the identity and control systems access, thus permitting the IOT system to record personnel identity and movements. In addition to allowing visiting personnel to work in a company through flexible security mechanisms, the proposed IOT system utilizes critical elements such as ZigBee sensors, an embedded system and RFID applications. Furthermore, each node displays information data from the interface, integrated with the ZigBee and RFID interface to monitor both the status of each node and the control region for precise measurement via the proposed PSO algorithms.

## Acknowledgments

This research was supported by the National Science Council of Taiwan under grant NSC 99-2220-E-167-001. The authors would like to thank the National Chin-Yi University of Technology, Taiwan for financially supporting this research.

## References

- [1] K.M. Passino, Biomimicry of bacterial foraging for distributed optimization and control, *IEEE Control Syst. Mag.* 22 (3) (2002) 52–67.
- [2] S. Appadwedula, V.V. Veeravalli, D.L. Jones, Energy efficient detection in sensor networks, *IEEE J. Sel. Areas Commun.* 23 (4) (2005) 693–702.
- [3] B.G. Jagyasi, B.K. Dey, S.N. Merchant, U.B. Desai, An mmse based weighted aggregation scheme for event detection using wireless sensor network, in: 14th European Signal Processing Conference, EUSIPCO 2006, pp. 132–137.
- [4] B.G. Jagyasi, B.K. Dey, S.N. Merchant, U.B. Desai, Weighted aggregation scheme with lifetime-accuracy tradeoff in wireless sensor network, in: Proc. 4th International Conference on Intelligent Sensing and Information Processing, 2006, pp. 1531–1537.
- [5] Y. del Valle, G.K. Venayagamoorthy, S. Mohagheghi, J.C. Hernandez, R. Harley, Particle swarm optimization: basic concepts, variants and applications in power systems, *IEEE Trans. Evol. Comput.* 12 (2) (2008) 171–195.
- [6] R. Blum, S. Kassam, H.V. Poor, Distributed detection with multiple sensors: part ii - advanced topics, *Proc. IEEE* 85 (1) (1997) 64–79.
- [7] W. Heinzelmal, A. Chandrakasam, H. Balakrishnan, An application specific protocol architecture for wireless micro sensor networks, *IEEE Trans. Wireless Commun.* 1 (4) (2002) 660–670.
- [8] Z. Chair, P.K. Varshney, Optimum data fusion in multiple sensor detection systems, *IEEE Trans. Aerosp. Electron. Syst.* 27 (1) (1986) 98–101.
- [9] Z. Chair, P.K. Varshney, Distributed Bayesian hypothesis testing with distributed data fusion, *IEEE Trans. Syst. Man Cybern.* 18 (5) (1988) 695–699.
- [10] B. Chen, R. Jiang, T. Kasetkasam, P.K. Varshney, Channel aware decision fusion in wireless sensor networks, *IEEE Trans. Signal Process.* 52 (12) (2004) 145–154.
- [11] J.-J. Xiao, S. Cui, Z.-Q. Luo, A.J. Goldsmith, Joint estimation in sensor networks under energy constraints, in: Proc. IEEE First Conf. Sensor and Ad Hoc Commun. and Networks, Santa Clara, CA, Oct. 2004, pp. 538–544.
- [12] L.F. Akyildiz, W. Su, Y. Sankarasubramaniam, E. Cayirci, A survey on sensor networks, *IEEE Commun. Mag.* (August) (2002) 1207–1211.
- [13] Wen-Tsai Sung, Employed BPN to multi-sensors data fusion for environment monitoring services, in: ATC 2009, in: LNCS, vol. 5586, Springer-Verlag, Berlin Heidelberg, 2009, pp. 149–163.
- [14] Wen-Tsai Sung, Hung-Yuan Chung, Design an innovative localization engines into WSN via ZigBee and SOC, in: 2008 CACS International Automatic Control Conference, Nov. 21–23, 2008, pp. 24–30.
- [15] Wen-Tsai Sung, Determine global energy minimum solution via Lyapunov stability theorem, *Int. J. Innovative Comput. Inf. Control (IJICIC)* 5 (7) (2009) 2011–2030.

- [16] A. Boukerche, H.A.B. Oliveira, E.F. Nakamura, A.A.F. Loureiro, Localization systems for wireless sensor networks, *IEEE Wireless Commun. Mag.* 14 (6) (2007) 6–12.
- [17] K. Romer, F. Mattern, The design space of wireless sensor networks, *IEEE Trans. Wireless Commun.* 11 (6) (2004) 54–61.
- [18] T. Wimalajeewa, S.K. Jayaweera, Optimal power scheduling for correlated data fusion in wireless sensor networks via constrained PSO, *IEEE Trans. Wireless Commun.* 7 (9) (2008) 3608–3618.
- [19] Juan A. Lazzús, Optimization of activity coefficient models to describe vapor–liquid equilibrium of (alcohol + water) mixtures using a particle swarm algorithm, *Comput. Math. Appl.* 60 (8) (2010) 2260–2269.
- [20] Chao Xing, Yanjun Li, Ke Zhang, Ling Wang, Shadow detecting using particle swarm optimization and the Kolmogorov test, *Comput. Math. Appl.* 62 (7) (2011) 2704–2711.
- [21] Shahram Jamali, Gholam Shaker, PSO-SFDD: defense against SYN flooding DoS attacks by employing PSO algorithm, *Comput. Math. Appl.* 63 (1) (2012) 214–221.
- [22] Wu Deng, Rong Chen, Jian Gao, Yingjie Song, Junjie Xu, A novel parallel hybrid intelligence optimization algorithm for a function approximation problem, *Comput. Math. Appl.* 63 (1) (2012) 325–336.